ACCELERATED SIMULATION OF NEAR-EARTH-ORBIT POLYMER DEGRADATION*

Eric Laue
Jet Propulsion Laboratory

ABSTRACT

There is a need to simulate the near-Earth-orbit environmental conditions, and it is useful to be able to monitor the changes in physical properties of spacecraft materials. This document presents two different methods for simulating the vacuum-ultraviolet (VUV) and soft X-ray near-Earth-orbit flux. Also, methods for monitoring the changes in optical ultraviolet transmission and mass loss are presented. The results of exposures to VUV photons and charged particles on these materials are discussed.

INTRODUCTION

The electromagnetic environment for near-Earth-orbit spacecraft is probably the most difficult to characterize since it ranges from the Earth's magnetic field through the radio-frequency, infrared, visible, ultraviolet (UV), X-ray, vacuum-ultraviolet (VUV), and extreme-ultraviolet (EUV) parts of the electromagnetic spectrum and out as far as high-energy cosmic rays. The 22-year solar cycle accounts for the wide variation in the EUV, X-ray, and particle environment. These fluxes can vary by orders of magnitude. Reference 1 contains a review of the trapped-radiation environment.

The recent return to Earth of the Long-Duration Exposure Facility (LDEF) has provided the opportunity to observe the effects of a 5-year exposure. Damage to spacecraft organic thermal blankets and to metallic surfaces has been observed. Simulation of these effects has been attempted by many different laboratories throughout the world.

This document reports on recent work at JPL that has resulted in two methods of exposure and two methods of in situ monitoring of changes in the sample undergoing exposure.

---

* The research described in this paper was carried out by the Jet Propulsion Laboratory, California Institute of Technology, under a contract with the National Aeronautics and Space Administration.

SIMULATION METHODS

The VUV photon source in the present work is provided by the Cathodeon[1] deuterium model VO1 lamp. Its spectrum and long-term performance have been studied by Hindsberg and Kanazawa (Ref. 2) of the British National Laboratory.

Reference 2 covers a study by the British National Laboratory of the spectrum and long-term performance of the Cathodeon deuterium model V01 lamp. Figure 1 is a plot of the solar spectral irradiance between l00 to 300 nm; Figure 2 is a comparison of the V01 lamp radiance to other available reference vacuum ultraviolet sources. The 124-nm line from the deuterium gas simulates the solar Lyman alpha line. The system shown in Figure 3 has been in use during a recent 9-month period. Figure 3 is a section view and block diagram of the 124-nm irradiation source. The system has been used to expose various polymers. A 20-day cycle has been found to be useful in that changes in weight and UV transmission can be measured. The changes in the characteristics of the sample undergoing 124-nm irradiation can be monitored by the change in transmission versus time for partially transparent samples or by the use of a quartz crystal macrobalance (QCM) for opaque materials.

During the Grand Tour work, a 2-ft diameter aluminum disc was installed in a 1.8-m vacuum chamber and charged up to l kV. This isolated disc retained its charge for 18 hours with only a 200-volt drop. When the 254-nm (low-pressure mercury vapor) source was used to illuminate the disc through a quartz window, the charge was dissipated in less than 1 hour. Based upon this effect, a second type of near-Earth-orbit simulator was developed. A sample of the material under test was installed in a 0.61-m-diameter vacuum chamber. A 4-watt, ozone-producing, mercury lamp was used to illuminate the sample. At the same time, a brush corona, at approximately 2 kV, was generated, which also illuminated the sample. The roughing pump's base pressure to approximately $1.4 \cdot 10^{-2}$ Pa. A small gas leak sets the nominal chamber pressure during exposure to approximately $3.4 \cdot 10^{-2}$ Pa. This combined irradiance (254-nm and corona) has been used to irradiate several samples. Figure 4 is a plot of the approximate corona current at the sample location versus chamber pressure. Figure 5 is a block diagram of the system.

Figure 6 is a photograph of the open tank showing the QCM and 10-cm-by-10-cm corona reference plate, while Figure 7 is a photograph showing the source details.

IN SITU MONITORING

Concurrent with the development of the sources, two different techniques to monitor changes in the material under test were developed. For the 124-nm source, a Hamamatsu[2] model R1132 phototube (spectral sensitivity from ll5 to 160 nm) was found to be effective. Since the specified bias is 15 volts, a battery bias supply is not a source noise and can be used without special precautions to avoid Paschen breakdown. A downward "drift" in sensitivity of the R1132 detector has been reported by Hamamatsu. Their source is a Krypton capillary discharge, and it

[1] Cathodeon Ltd., Nuffield Rd., Cambridge, England.
[2] Hamamatsu Corp., San Jose, CA

develops a 6-nA current in the diode. In the system at JPL, the diode current is 0.05 nA. Monitoring the 254-nm irradiation is accomplished using either a 7–54 nickel-cobalt glass filter or a 260-nm filter in conjunction with a Hamamatsu GaAsP model G1126-02 photovoltaic cell.

Recently, the IBM New Almaden Research Center[3] has developed a technique for driving quartz crystals whose mechanical load has degraded the Q of the crystal several orders of magnitude (Ref. 3). The conversion from frequency change to mass loss involves many assumptions. In reporting such conversions, a careful listing of these assumptions will avoid false interpretation of the data. References 4 and 5 discuss some facets of these assumptions. A test using Dykem, a cellulose-acetate-based dye, has revealed the effects of irradiation by the 254-nm source on mass loss, the corona's mass loss characteristics, and the mass loss resulting from the combined sources. Figure 8 is a plot of frequency versus time and Figure 9 is a computed frequency-change-per-hour for the three different conditions of exposure. Figure 10 shows the loss in weight and change in transmission of an FEP sample exposed in the 254-nm and corona system, while Figure 11 shows the change in frequency of a QCM for a white dot of the paint such as is used for spacecraft at JPL. This represents the loss in mass of the paint.

During the development of these irradiation sources and monitoring techniques, certain procedures were found to be valuable. Measurement without the samples before and after the sample test will, 1), verify source and detector stability during the sample exposure and, 2), provide a baseline to quantify sample transmission. Secondly, an 18- to 24-hour conditioning period before starting irradiation allows the effects of evacuation or moisture loss to settle down.

SAMPLE EVALUATION TECHNIQUES

The major advantage to laboratory simulation rests in the fact that it is possible at any time to interrupt the exposure and perform a variety of analytical measurements on the samples. The following is a brief discussion of sample evaluation techniques, with some comments as to their limitations and approximate resolution.

1. The film samples are clamped between two aluminum rings whose dimensions are 2.54 cm for inside diameter and 3 cm for outside diameter. The films are nominally 0.0051 cm (0.002 in.) thick. The initial mass of the films is 0.1 gm and the weighing resolution 0.0001 gm. The change in mass after an exposure can be measured.

2. The change in UV and visible transmission can be measured. Measurement in the VUV would be more useful, but is much more difficult to accomplish.

3. Infrared transmission (FTIR) was used to monitor any changes in the existing absorption bands or the appearance of new absorption bands and to provide information on changes in the molecular structure of the sample.

[3] IBM New Almedan Research Lab., San Jose, CA

4. Comparison of an unexposed sample with the exposed sample using a scanning electron microscope can provide insight into the nature of the surface after exposure; however, the application of the required conducting surface on the samples would prevent additional exposures.

5. Because of the ability to measure the 4-MHz basic frequency to 1 Hz and, under ideal conditions, to 0.1 Hz, the QCM technique is used to measure sample changes during exposure. Using the information from Ref. 2, the "K" for 4 MHz is 1.13 angstroms/ Hz. Assuming that the sample has a density of 1, the resolution is 10 E^{-8} gms. Since, on occasion, the load is a small dot in the center of the crystal, the results indicated in Ref. 5 should be considered. Thus, any quantitative calculations have an uncertainty of $\pm$30 percent. Figure 12 is a comparison of the spectral transmission of a reference versus a 40-day exposure of demetallized 0.5-mil Mylar. Figure 13 is the spectral transmission of 2-mil FEP after a 40-day exposure. This was a repeat of the exposure used for Figure 10.

6. The Atomic Force Microscope (AFM) allows the measurement of the surface of materials on an atomic scale. Figure 14 shows the AFM scan of an FEP sample from the LDEF spacecraft and a similar sample which had been exposed for 40 days in the 254-nm and corona irradiation source. While the laboratory-exposed sample does not exhibit a depth of erosion as great as the LDEF sample, the similarity is obvious. The LDEF sample was exposed for approximately 5000 hours. The 254-nm and corona exposure was 960 hours, an acceleration of approximately five times the near-Earth-orbit environment.

CORONA CHARACTERIZATION

The corona voltage source is a 13.5-kV power supply with a 15-MΩ series resistor to control the current. It is possible to reverse the polarity of the corona electrode voltage with respect to the chamber and sample ground. When the corona electrode is negative, its potential is −4.4 kV. The voltage drop across the 15 MΩ is 9.1 kV. The corona electrode current is 0.6 mA. With a positive electrode, the potential is only 2.3 kV and the current is 0.75 mA.

A description of the nature of the corona in terms of the energy distribution and particles generated in the bleed air would be desirable. In the present system this is not feasible. Instead, a 2-cm-by-2-cm CRES electrode was installed in place of the normal samples and used as a Langmuir probe by monitoring the current as the probe was biased between a plus and a minus voltage (with respect to the chamber ground).

Figure 15 is a plot of electrode current versus bias voltage with the corona source at a negative potential with respect to the chamber ground. This appears to be a normal diode curve, except that if a bias voltage greater than 120 V is applied, the observed current exhibits instability and appears to "run away". Figure 16 is a plot of the $\mu A \cdot cm^{-2}$ with a positive voltage on the corona electrode. While this appears to be a "diode type" curve, it requires a bias potential greater than 100 V before the current changes polarity. One plausible explanation for the nature

of the positive-biased source could be that the collisions between the ionized gas and the neutral molecules are producing electrons and gamma-ray particles. With the positive potential on the corona source, a blue glow is present on the corona electrode and there is a10-percent increase in the current from a GaAsP diode +7–54 filter monitor. The percentage distribution in 20-V bins is shown in Figure 17. This data was generated by weighing the total curve and the weight of the 20-V segments. Apparently, an observable percentage of the current between 0 and +100 V still are positively charged particles.

CONCLUSIONS

There is no claim that this system accurately reproduces the fields and particles in the air mass zero environment. Nevertheless, the ability to remove and evaluate samples from the system, then continue the exposure has been useful. Changes in sample characteristics have been observed for all of the materials except metallized Mylar.

The system is reasonably simple to set up and, when stabilized after the first 24 hours, can function unattended except for a daily monitoring of the system parameters.

REFERENCES

[1] E.G. Stassinpoulos and J.P. Raymond, Proceedings of the IEEE, vol. 76, no. 11, p. 1423, Nov. 1988.

[2] W.D. Hindsberg and K.K. Kanazawa, Rev. Sci. Instru., vol. 60, no. 3, p. 489, Mar. 1989.

[3] P.J. Key and R.C. Preston, J. Physics E: Sci. Instru., vol. 13, p. 866, Great Britain, 1980.

[4] C.E. Reed., K.K. Kanazawa, and H. Kaufman, J. Appl. Phys., vol. 68, no. 5, p. 1993, Sept. 1990.

[5] P.J. Cumpson and M.P. Seah, Meas. Sci. Technol., vol. 1, p. 544, 1990.

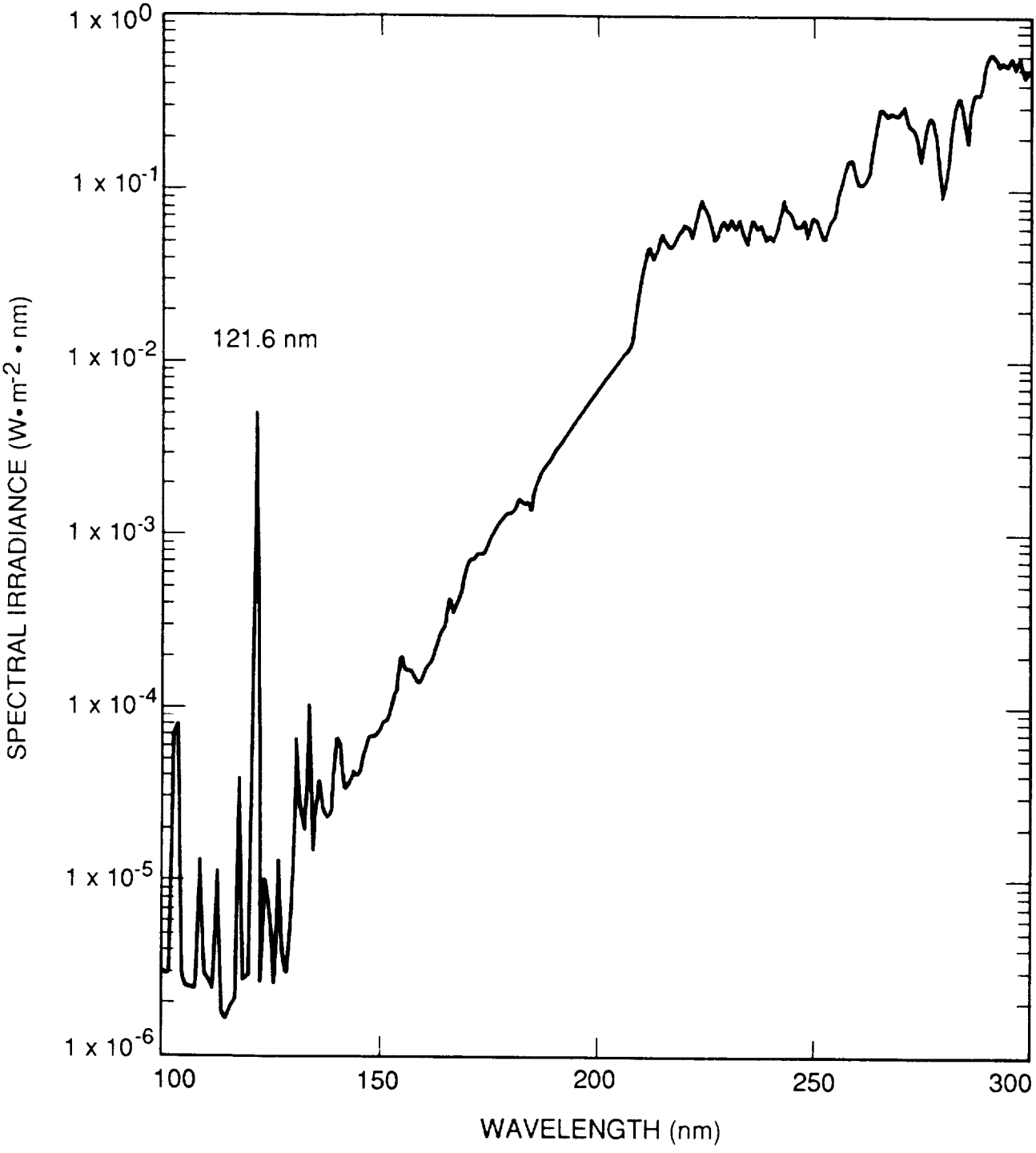

Figure 1. Air Mass Zero Solar Spectrum

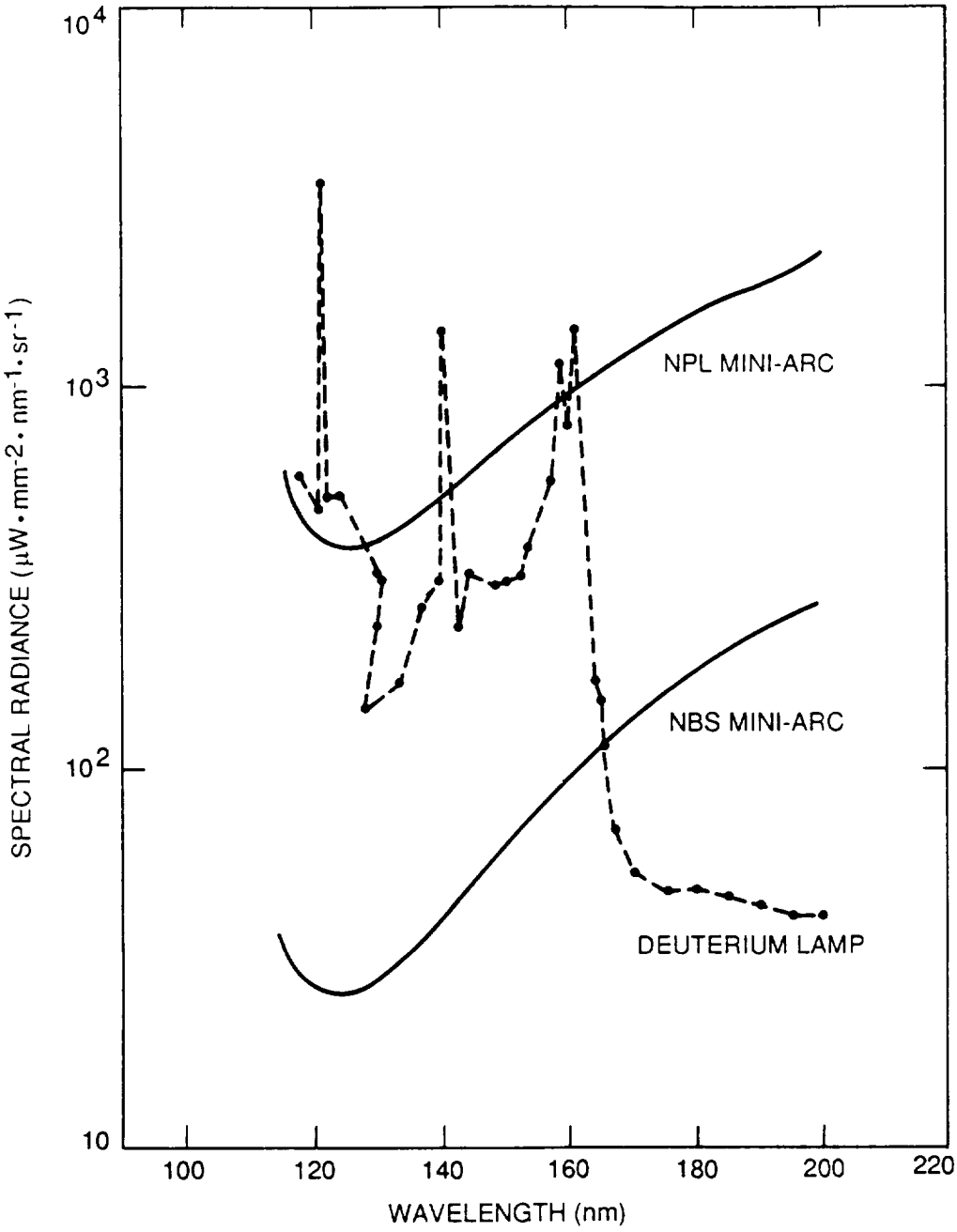

Figure 2. Radiance Levels of Cathodeon V01 Lamp

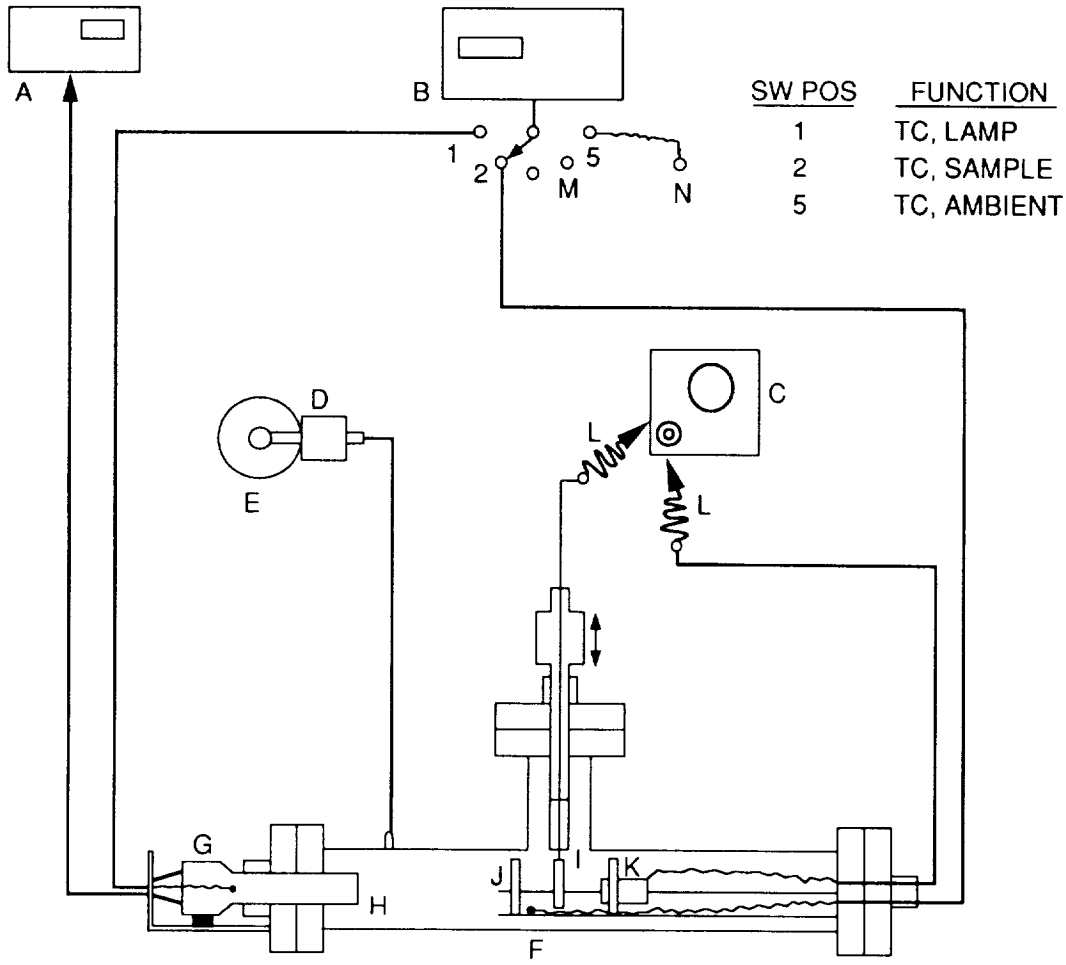

LEGEND:

A. CATHODEON LAMP POWER SUPPLY, LAMP VOLTAGE AND CURRENT (mA)
B. CER 003 ANALOGIC* TEMPERATURE
C. ELECTROMETER
D. OIL VAPOR FILTER
E. VACUUM PUMP
F. THERMOCOUPLE, SAMPLE
G. THERMOCOUPLE, LAMP
H. VO1 VUV LAMP
I. COPPER DISK
J. SAMPLE
K. CsI VUV PHOTODIODE
L. BNC PLUG
M. SWITCH
N. THERMOCOUPLE, AMBIENT

* ANALOGIC CORP., PEABODY, MA

Figure 3. Section View and Block Diagram of 124-nm Irradiation Source

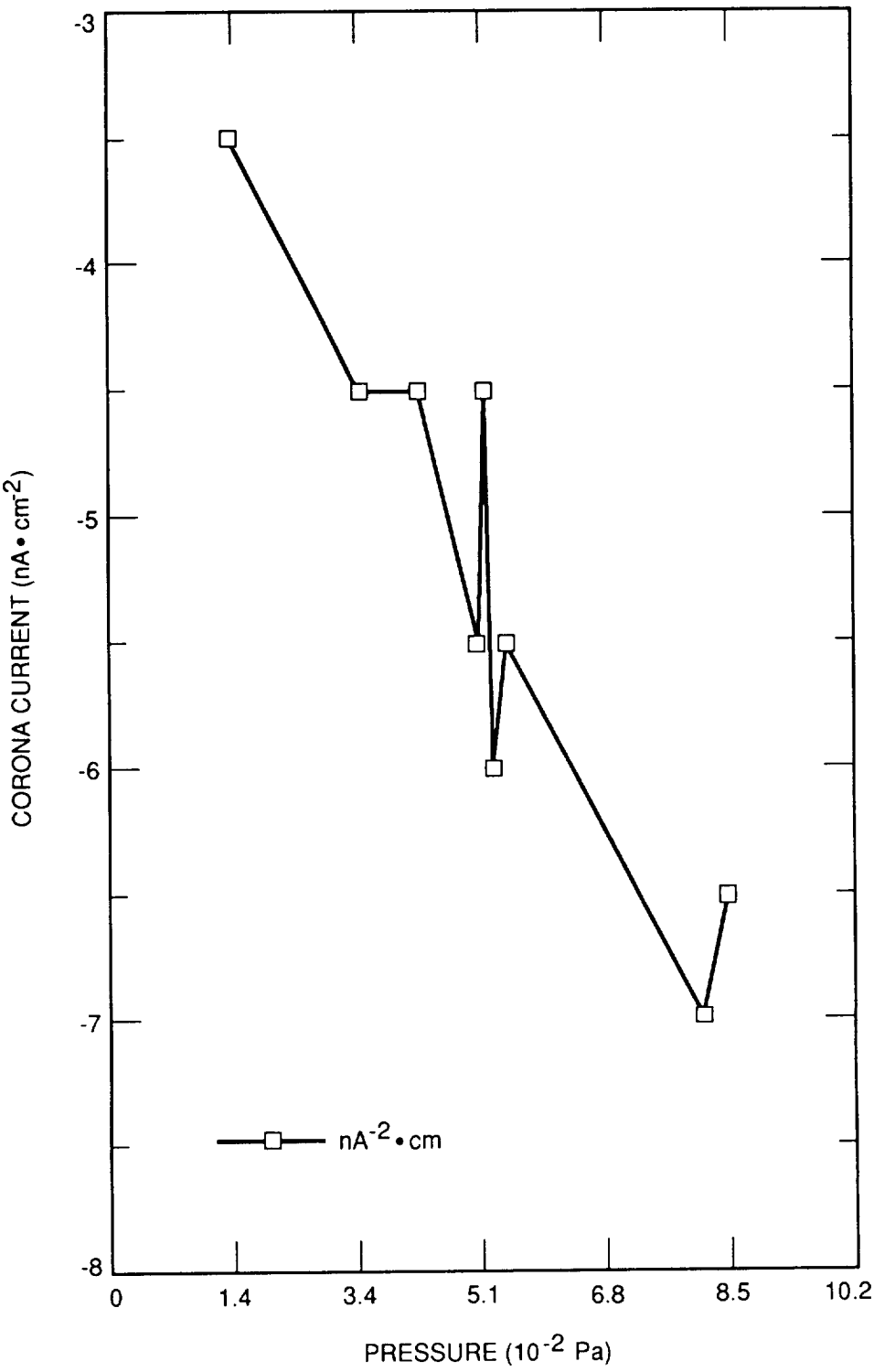

Figure 4. Corona Current Versus Chamber Pressure

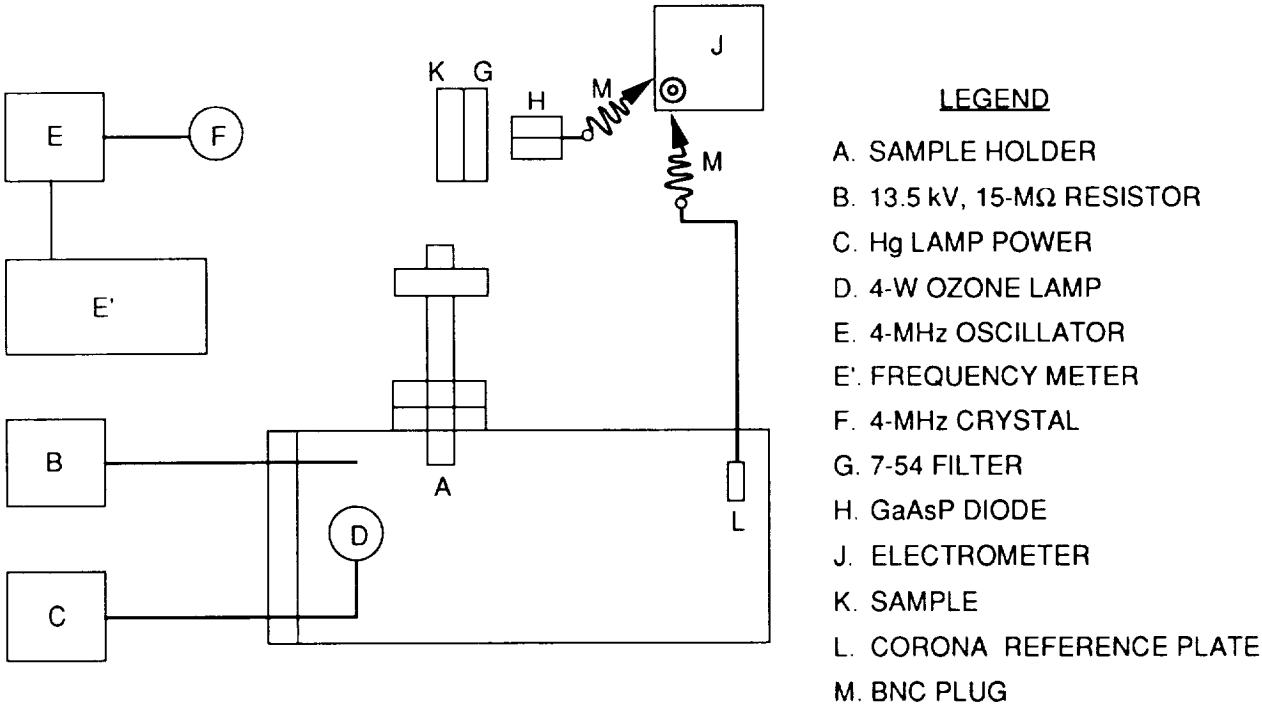

Figure 5. Block Diagram of 254-nm and Corona Irradiation Source

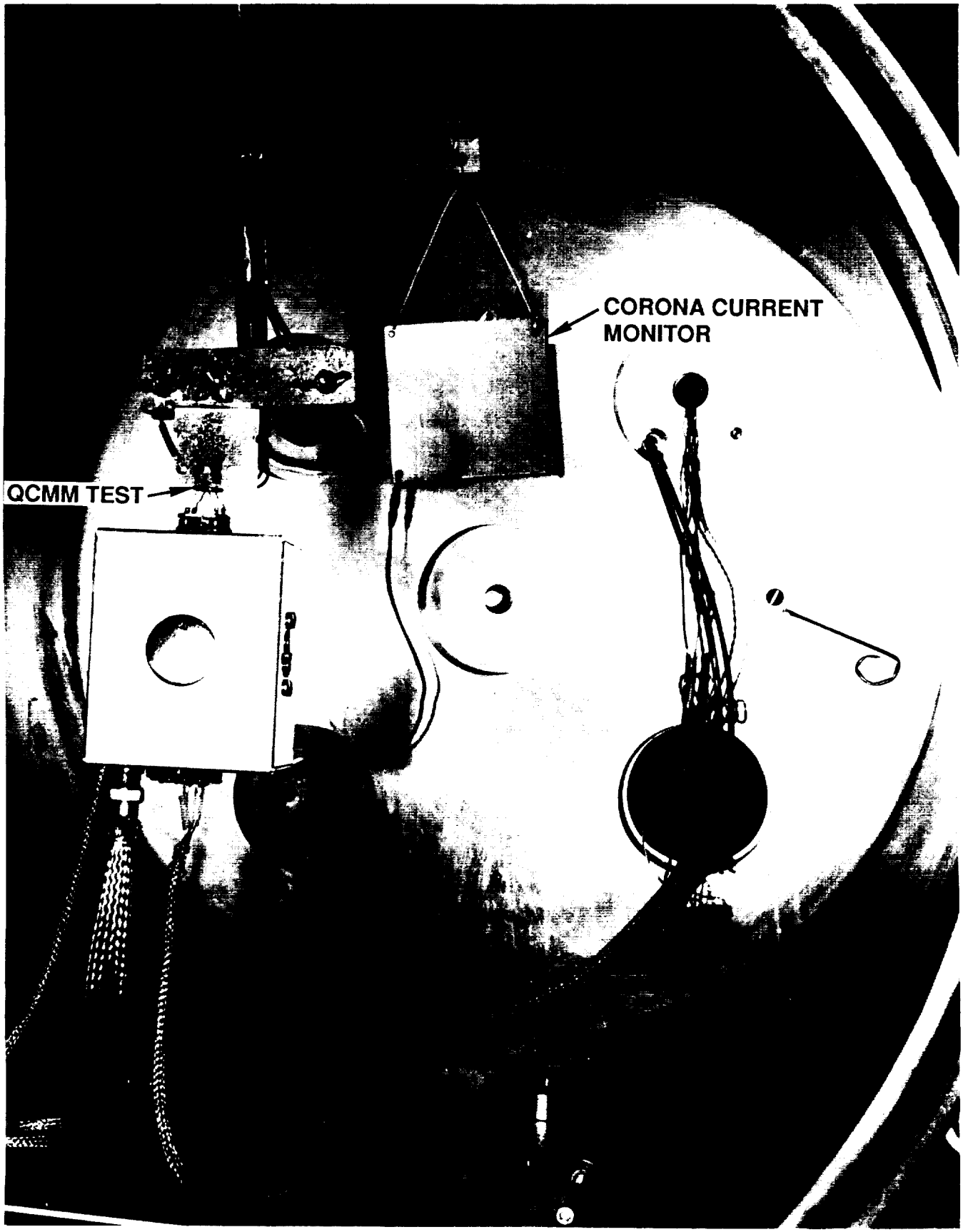

Figure 6. Photograph of 254-nm and Corona Irradiation Tank (JPL-15329B)

Figure 7. Photograph of 254-nm and Corona Irradiation Source (JPL-15329A)

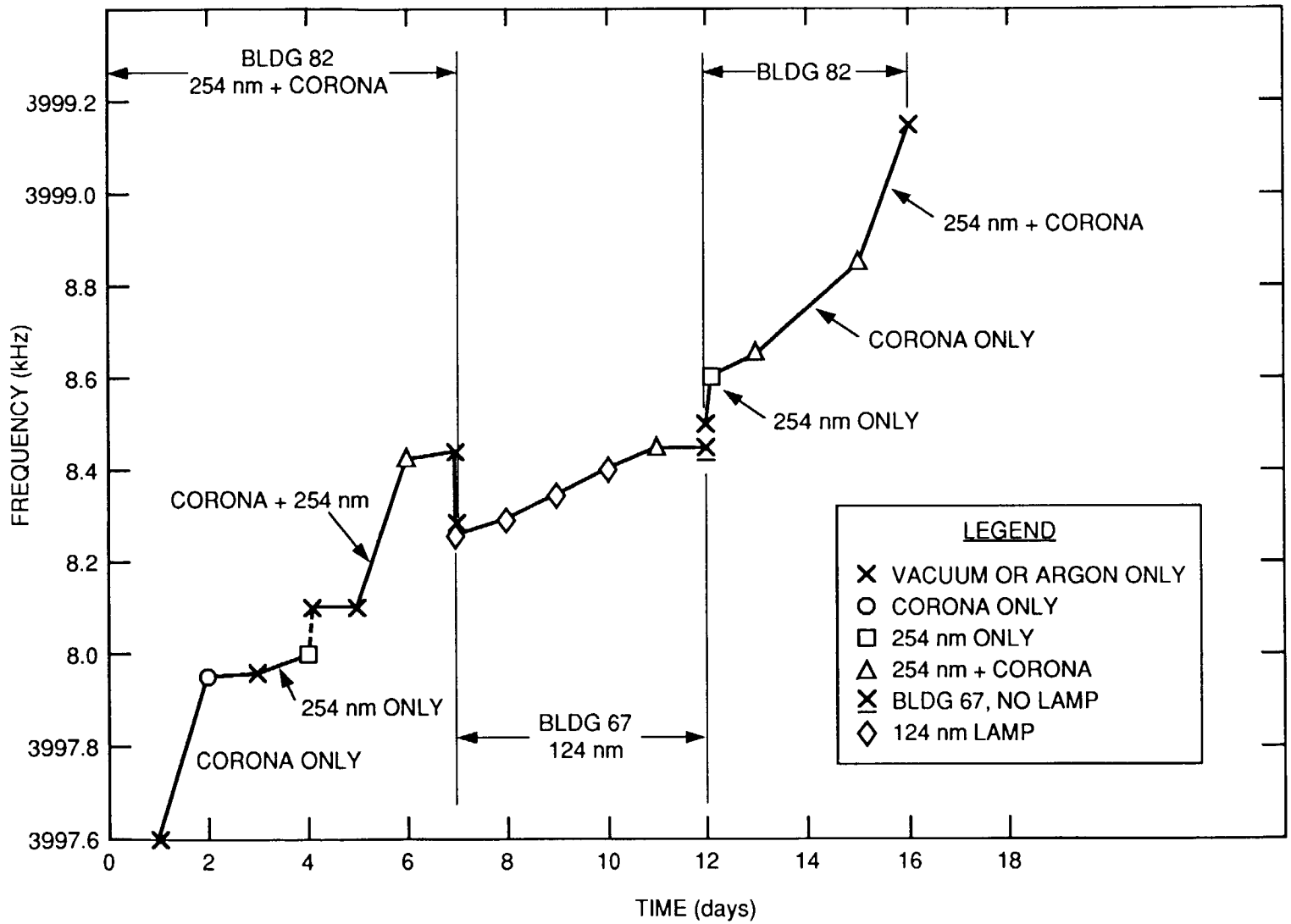

Figure 8. Plot of Dykem Sample Crystal Frequency Versus Time

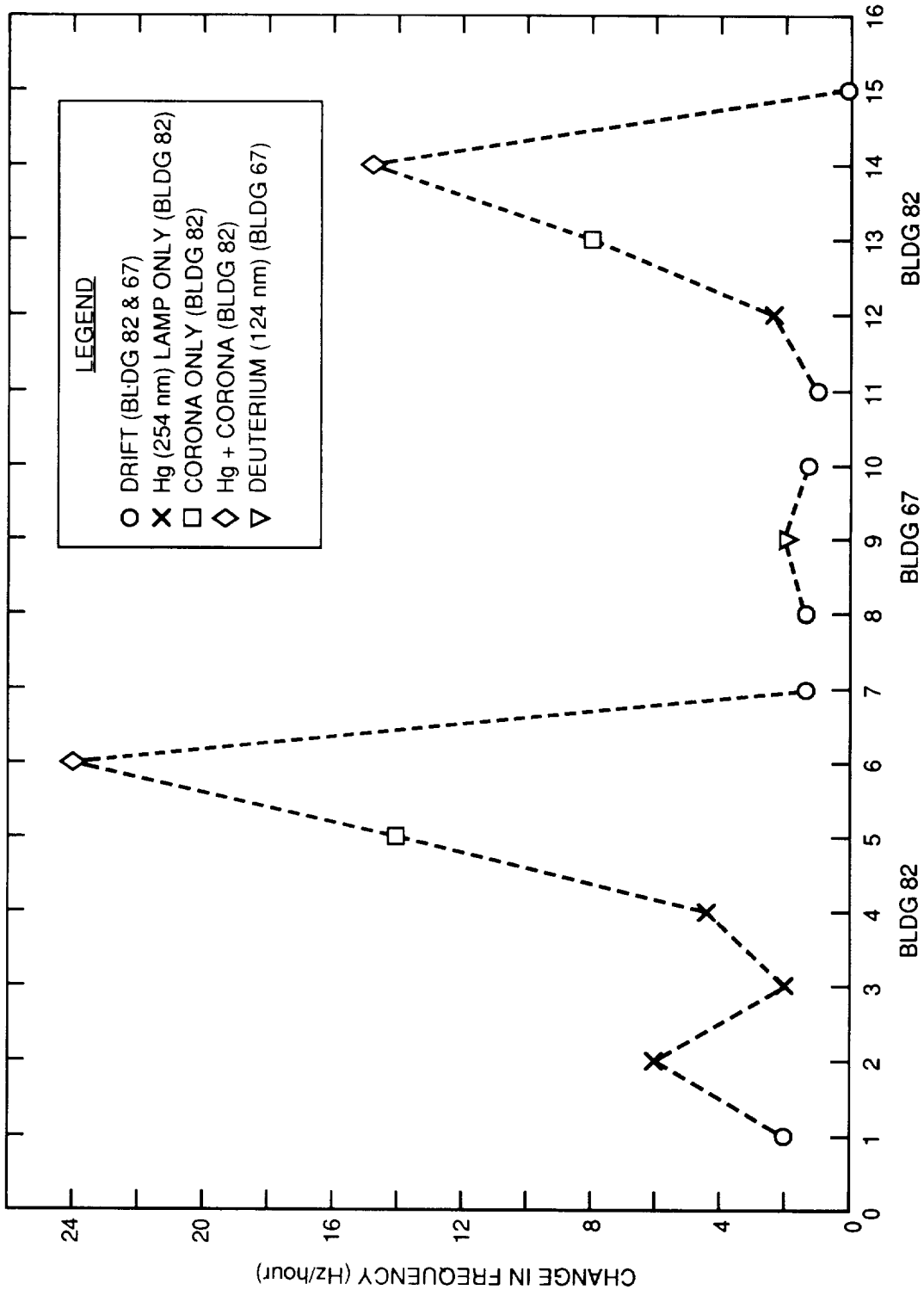

Figure 9. Dykem Sample Frequency Rate of Change

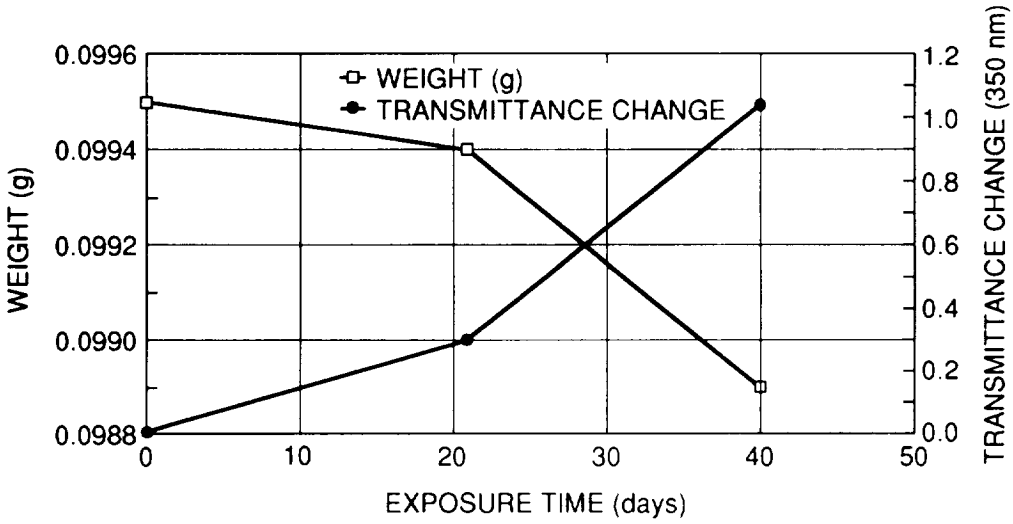

FEP-VUV EXPOSURE

	124 nm EXPOSURE	WEIGHT (g)	TRANSMITTANCE CHANGE
1)	0	0.0995	0
2)	21	0.0994	0.3
3)	40	0.0989	1

Figure 10. FEP Mass Loss and Spectral Transmission

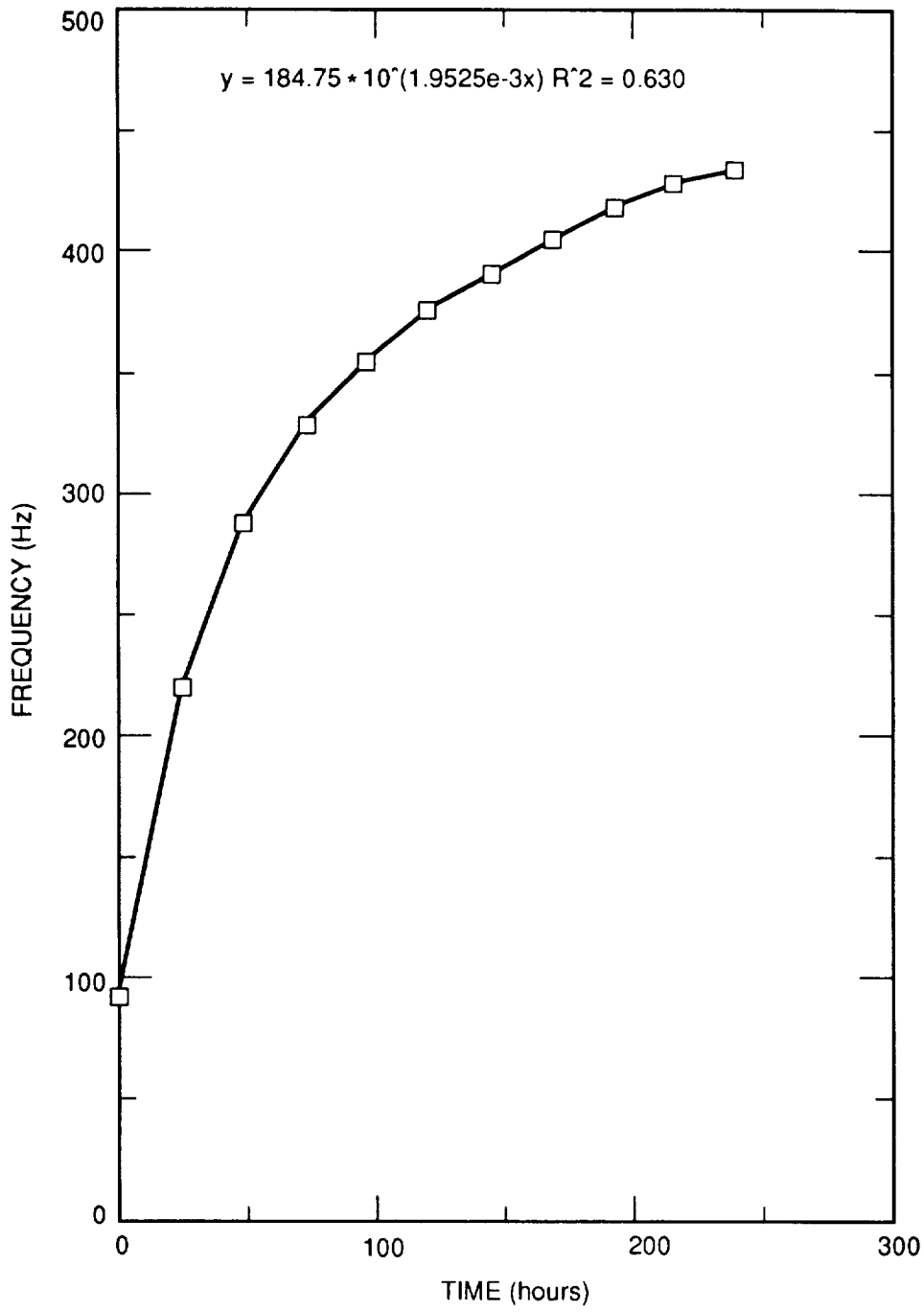

Figure 11. Plot of Frequency Versus Time, White Epoxy Sample, 254-nm and Corona Irradiation Source

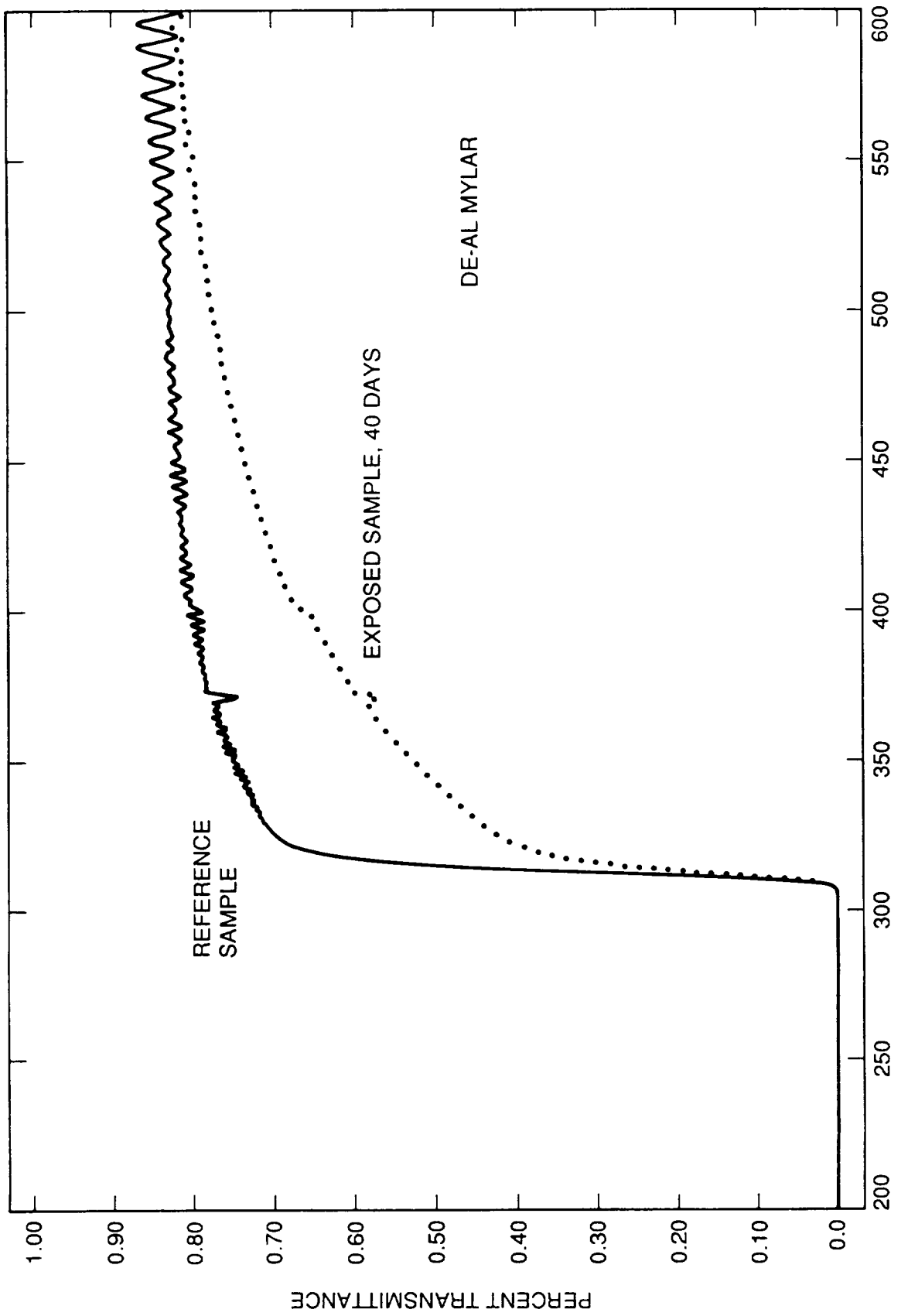

Figure 12. DE-AL Mylar Spectral Transmission

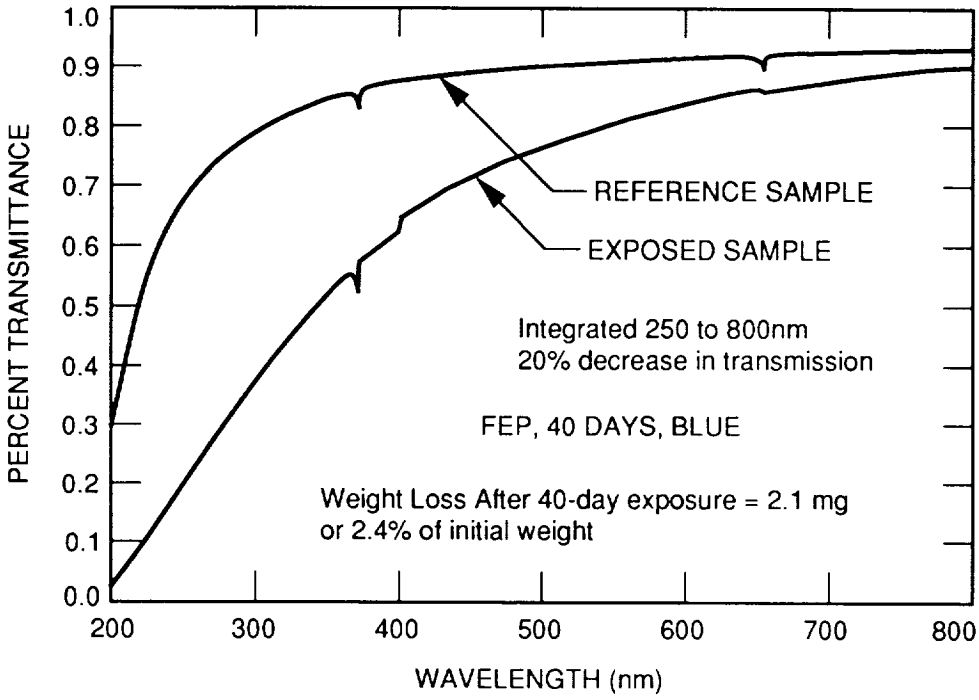

Figure 13. Spectral Transmission of 0.002-mil FEP After 40-Day Exposure

a. LDEF Sample
SEM Scan

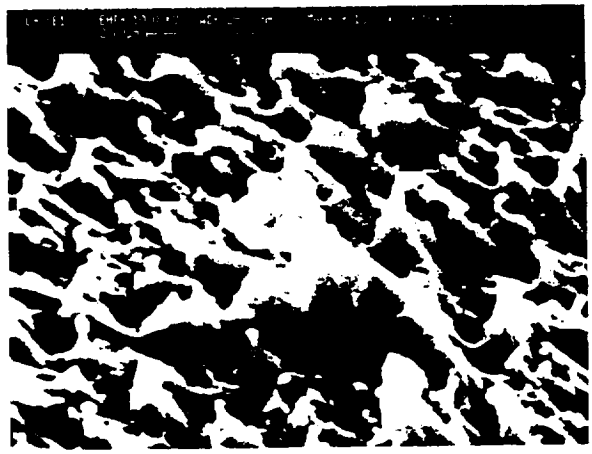

b. LDEF Sample
AFM Scan

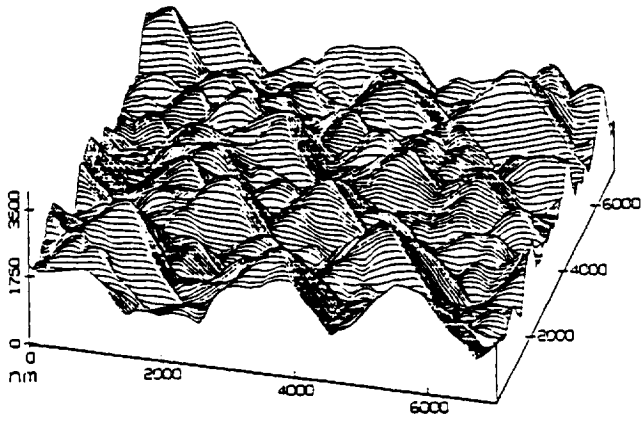

c. 40-Day-Exposure Sample,
254-nm and Corona
Irradiation Source

AFM Scan

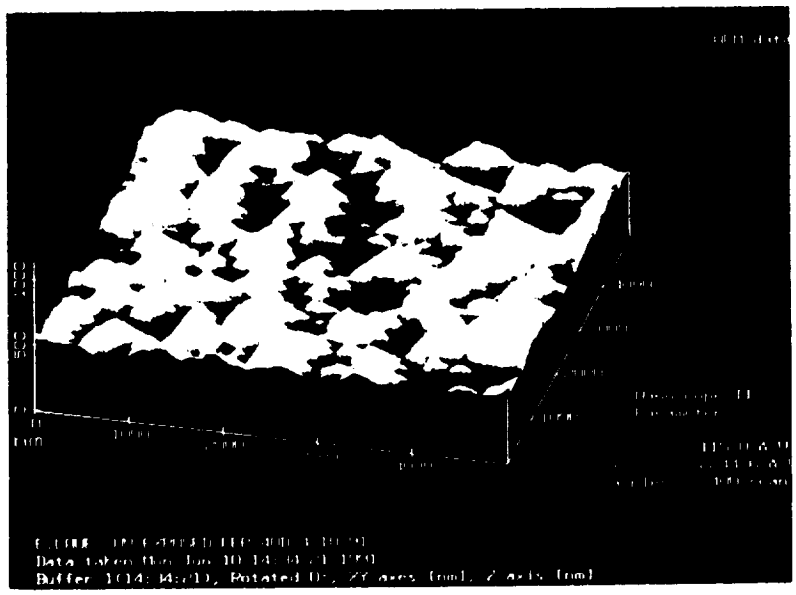

Figure 14. Scans of LDEF FEP Sample (a. and b.)Versus FEP 40-Day-Exposure Sample (c.), 254-nm and Corona Irradiation Source

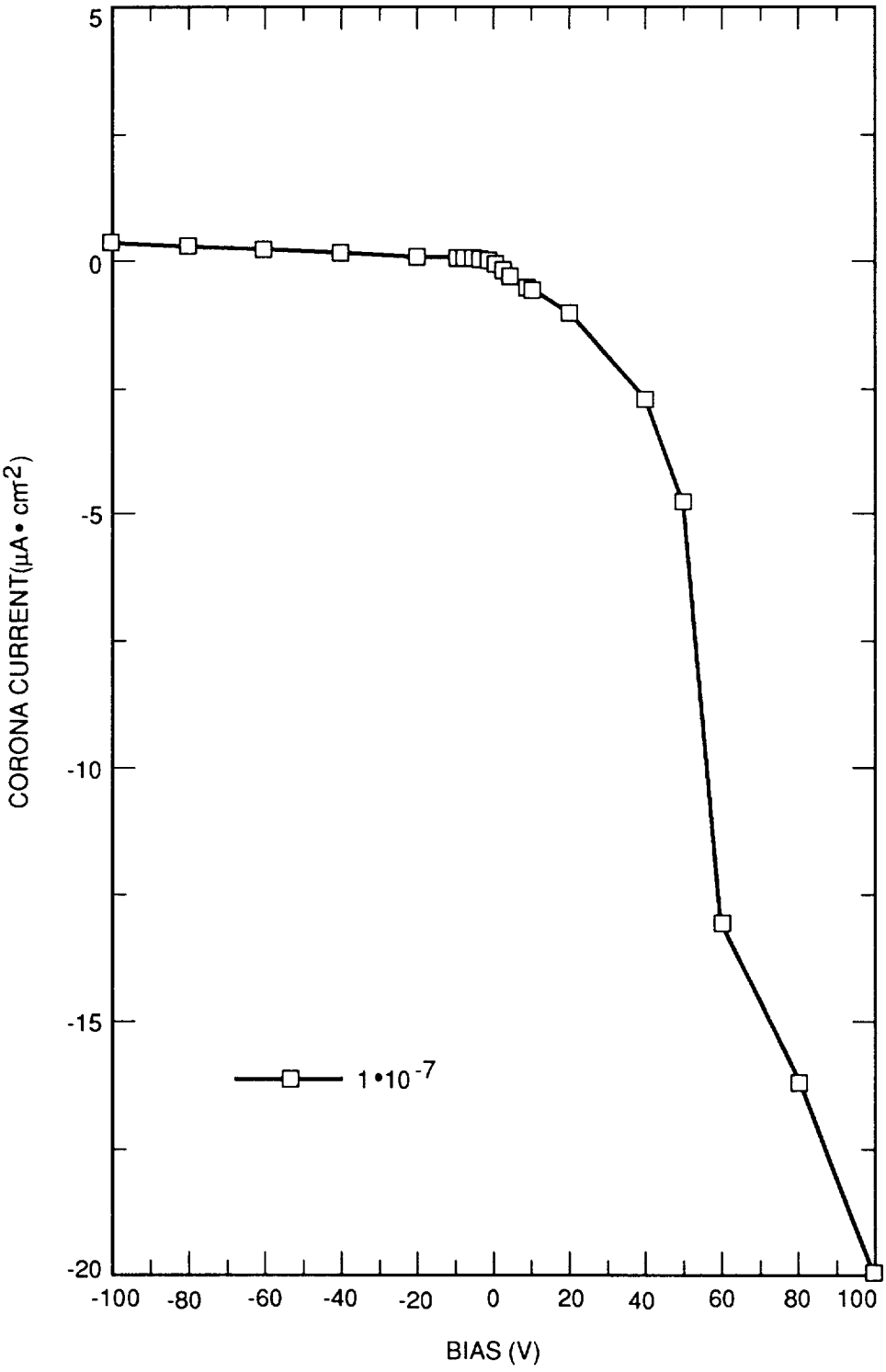

Figure 15. Plot of Current Versus Bias Voltage, –4.4-kV Corona

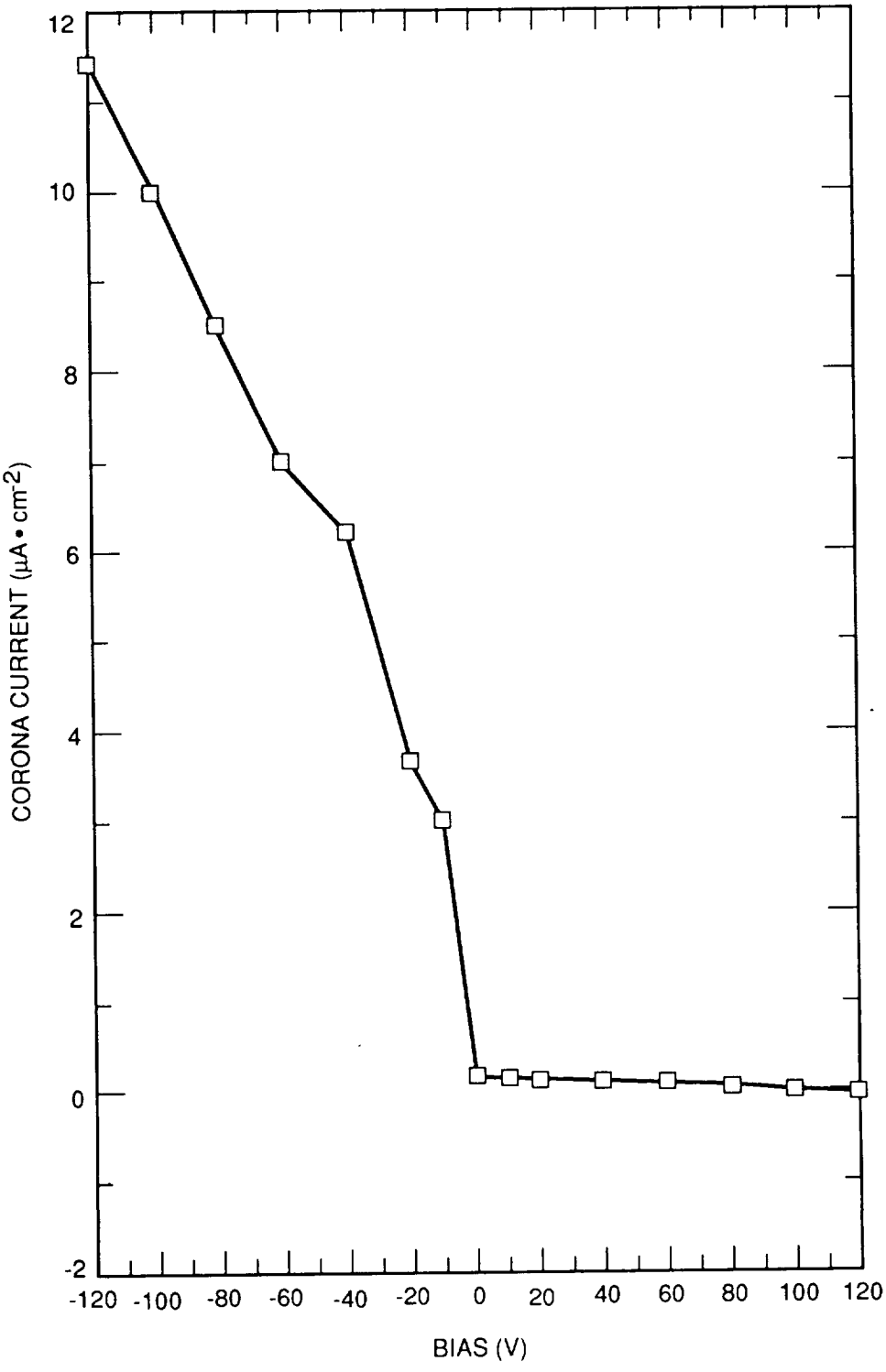

Figure 16. Plot of Current Versus Bias, +2.3-kV Corona

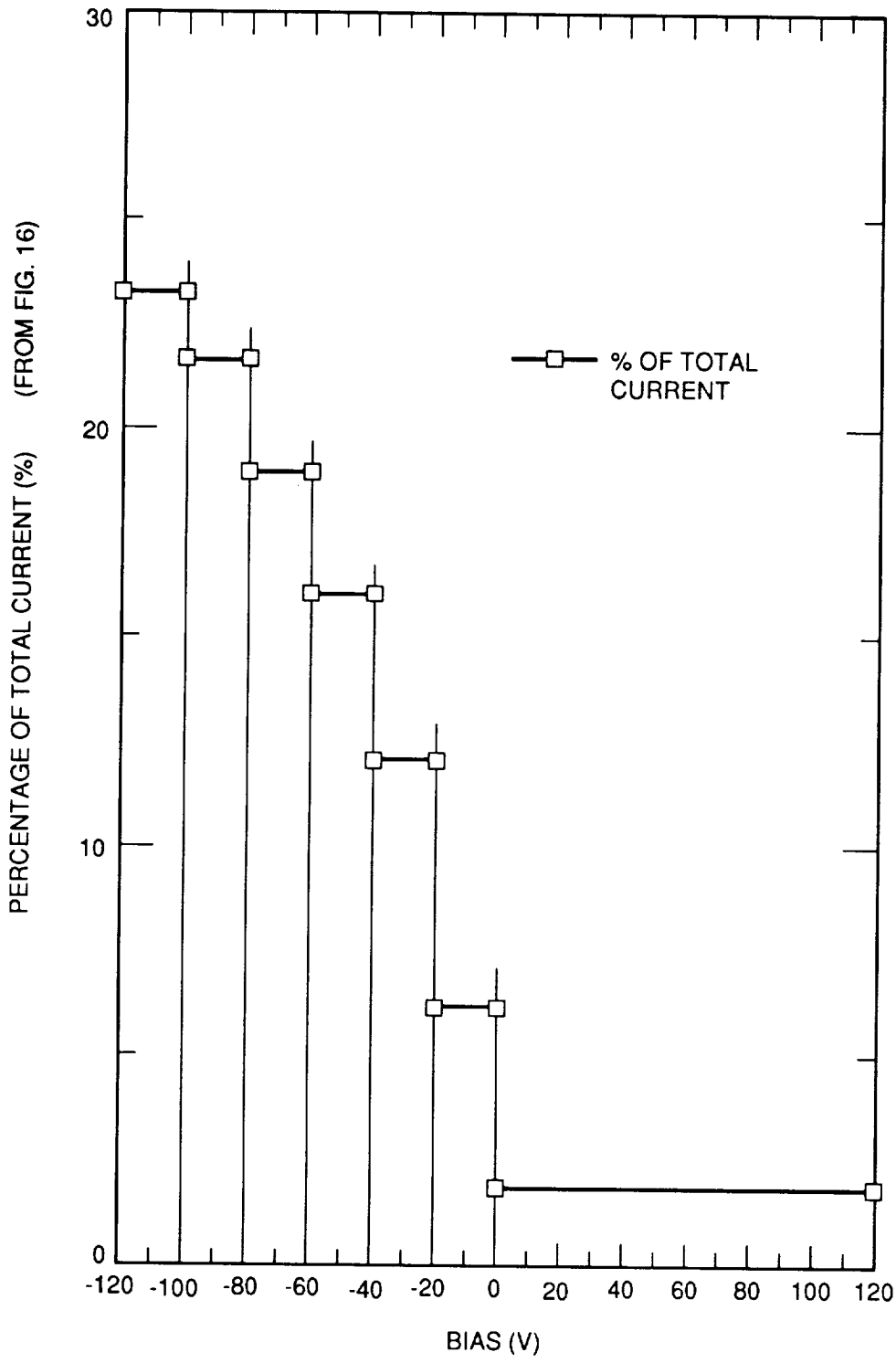

Figure 17. Percentage of Total Current Versus Bias